

# SiO<sub>2</sub>-Al<sub>2</sub>O<sub>3</sub> metastable phase equilibrium diagram without mullite

SUBHASH H. RISBUD\*, JOSEPH A. PASK

*Materials and Molecular Research Division, Lawrence Berkeley Laboratory and Department of Materials Science and Mineral Engineering, University of California, Berkeley, California 94720, USA.*

A metastable binary phase diagram between SiO<sub>2</sub> (cristobalite) and  $\alpha$ -Al<sub>2</sub>O<sub>3</sub> (corundum) in the absence of any mullite phase is presented. A eutectic is indicated at a temperature of  $\approx 1260^\circ\text{C}$  and a composition of  $\approx 18\text{ wt } \%$  ( $\approx 12\text{ mol } \%$ ) Al<sub>2</sub>O<sub>3</sub>. The liquidus of the proposed metastable system were positioned on the basis of the thermodynamic data calculated from the stable equilibrium diagram of Aksay and Pask [2]. Experimental evidence is also presented. A SiO<sub>2</sub>-Al<sub>2</sub>O<sub>3</sub> melt containing 80 wt % Al<sub>2</sub>O<sub>3</sub> cooled at a slow rate in sealed molybdenum crucibles shows crystalline Al<sub>2</sub>O<sub>3</sub> plus a glass phase whose composition followed the calculated extension of the stable Al<sub>2</sub>O<sub>3</sub> liquidus to lower temperatures. Compacts of cristobalite-corundum mixtures were fired at subsolidus temperatures to estimate the eutectic temperature experimentally. The proposed metastable phase diagram effectively explains the formation of non-crystalline phases in subsolidus reactions, and microstructure obtained on solidification of high alumina melts.

## 1. Introduction

Phase diagrams indicate the location of stable equilibrium phase boundaries and do not, in general, include data on metastable equilibria. In many systems, especially those forming glasses, kinetic inaccessibility of stable phases makes metastability readily realizable under normal experimental conditions. Development of metastable diagrams for such systems is, therefore, of importance in understanding solid state reaction sequences as well as of practical utility.

In their studies on phase equilibria in the SiO<sub>2</sub>-Al<sub>2</sub>O<sub>3</sub> system, (Fig. 1) Davis and Pask [1] and Aksay and Pask [2] suggested the existence of a metastable SiO<sub>2</sub>-Al<sub>2</sub>O<sub>3</sub> phase diagram in the absence of any mullite phase. The occurrence of amorphous phases in solid state reactions between cristobalite and alumina has been reported by several authors. Wahl *et al.* [3] observed by high temperature X-ray diffraction reactions at temperatures as low as 1200°C with no mullite formation. Subsolidus formation of non-crystalline

material was also reported by Staley and Brindley [4] in cristobalite-corundum reactions at 1500°C. Kennard *et al.* [5] observed microstructures containing only glass plus alumina during directional solidification of high alumina compositions.

The purpose of this study was to obtain by experimental and thermodynamic methods the metastable phase boundaries in the SiO<sub>2</sub>-Al<sub>2</sub>O<sub>3</sub> system that occur without precipitation of the mullite phase.

## 2. Procedures

### 2.1. Thermodynamic calculations

Using thermodynamic models [6–9] based on regular solution approximations, the activities of Al<sub>2</sub>O<sub>3</sub> were calculated along the Al<sub>2</sub>O<sub>3</sub> liquidus curve of the stable phase diagram (Fig. 1). The equation for calculating the activities takes the form:

$$\log_{10} a^L = \frac{\Delta H_M}{4.575} \left[ \frac{1}{T_M} - \frac{1}{T_L} \right] = \log_{10} a^S \quad (1)$$

\*Now at Department of Metallurgy and Materials Engineering, Materials Research Center, Lehigh University, Bethlehem, Pa 18015, USA.

where  $a^L$  = activity of the liquid in the liquidus composition referred to pure liquid standard state,  $a^S$  = activity of solid at the liquidus temperature referred to pure liquid standard state,  $\Delta H_M$  = heat of melting in cal mol<sup>-1</sup>,  $T_M$  = melting temperature in K, and  $T_L$  = liquidus temperature in K.

The main assumptions in the calculation procedure were the constancy of the heat of fusion with temperature, and ideality in the solution mixing of high temperatures. Further, assuming that the partial molal heat of solution of Al<sub>2</sub>O<sub>3</sub>,  $\overline{\Delta H}_{Al_2O_3}$ , is independent of temperature [9] over the temperature range of interest, the activity data obtained from Equation 1 were used to calculate isothermal activity coefficients of Al<sub>2</sub>O<sub>3</sub> at any chosen temperature  $T$ . Thus,

$$\Delta H_{Al_2O_3} = RT_L \log_{10} \gamma_L = RT \log_{10} \gamma_T \quad (2)$$

where  $T_L$  and  $\gamma_L$  are liquidus temperature and activity coefficients at the liquidus, respectively,  $T$  and  $\gamma_T$  are the temperature and activity coefficients at the chosen temperature  $T$ , and  $R$  is the gas constant (1.98 cal mol<sup>-1</sup> K<sup>-1</sup>); and

$$\log_{10} a_L = \log_{10} \gamma_{10} X \quad (3)$$

where  $X$  is the Al<sub>2</sub>O<sub>3</sub> mole fraction between 0.4 and 1.0 (liquidus compositions). The isothermal activity coefficients of Al<sub>2</sub>O<sub>3</sub> were fitted by the method of least squares to yield an expression of the form:

$$\log_{10} \gamma_T = A + BX + CX^2 + DX^3 \quad (4)$$

where  $X$  is the mole fraction of Al<sub>2</sub>O<sub>3</sub> and  $A$ ,  $B$ ,  $C$  and  $D$  are constants. Assuming that the fit represented by Equation 4 is valid for Al<sub>2</sub>O<sub>3</sub> mole fractions,  $X$ , less than 0.4 (Fig. 1)  $\log_{10} \gamma_T$  values at chosen mole fractions  $X$ , (between 0.15 and 0.34) were obtained. The activity coefficients at the liquidus temperature were then calculated from Equation 2. Using these calculated values of  $\log_{10} \gamma_T$  in Equations 1 and 3, the liquidus temperature at each Al<sub>2</sub>O<sub>3</sub> mole fraction,  $X$ , (0.15 <  $X$  < 0.35) was calculated. Similar calculations were performed for extension of the SiO<sub>2</sub> liquidus (Fig. 1) to lower temperatures.

## 2.2. SiO<sub>2</sub>–Al<sub>2</sub>O<sub>3</sub> melts

High purity fused silica\* and reactive  $\alpha$ -Al<sub>2</sub>O<sub>3</sub>† powders were blended in isopropyl alcohol, dried at  $\approx 110^\circ$  C, and calcined in a platinum crucible at  $\approx 600^\circ$  C for 12 h. Calcined mixtures containing 80 wt % Al<sub>2</sub>O<sub>3</sub> were pressed into molybdenum crucibles ( $\approx 11$  mm diameter by 15 mm height) which were then sealed around the lid by electron beam welding and helium leak-checked [10]. The sealing and leak-checking procedures were necessary to prevent loss of silica by vaporization during the high temperature melting. The sealed crucibles were heat treated in a tantalum resistance furnace‡ at a temperature of  $\approx 1985^\circ$  C under a vacuum of  $\approx 10^{-6}$  Torr. The furnace temperature was electronically controlled through the use of a W5Re–W26Re thermocouple (accuracy  $\pm 7^\circ$  C at 1800° C). In addition, the crucible temperature was monitored by an optical pyrometer (accuracy  $\pm 10^\circ$  C at 2000° C) utilizing black body conditions [2]. The pyrometers were calibrated against a NBS secondary standard pyrometer at the melting points of platinum (1772° C) and Al<sub>2</sub>O<sub>3</sub> (2054° C). All temperatures reported are based on the 1968 International Practical Temperature Scale (IPTS-68).

## 2.3. Cristobalite–alumina mixtures

The same high-purity fused silica powder that was used for preparation of the melts was heated in platinum crucibles in air at  $\approx 1420^\circ$  C for 7 days to obtain the cristobalite phase. Cristobalite–alumina batches were dry-milled and cold-pressed into pellets. The pressed compacts were fired in platinum crucibles in air at temperatures ranging from 1100 to 1280° C for various times. The diameters of the pellets before and after firing were accurately measured to obtain shrinkage data.

## 2.4. Materials characterization

Crystalline phases obtained after heat treating the SiO<sub>2</sub>–Al<sub>2</sub>O<sub>3</sub> melts and the cristobalite–corundum pellets were identified by X-ray diffraction using silicon§ as an internal standard after crushing specimens to a powder.

\*— 325 mesh Corning 7940 silica, Corning Glass Works, NY (free from metallic impurities).

† Aluminum Co. of America, Pittsburgh, Pa. Chemical analysis (wt %) Na<sub>2</sub>O 0.08, SiO<sub>2</sub>, 0.05, CaO 0.03, MgO 0.05, Fe<sub>2</sub>O<sub>3</sub> 0.01, MnO 0.0015, B<sub>2</sub>O<sub>3</sub> < 0.001, Cr<sub>2</sub>O<sub>3</sub> 0.0002.

‡ Richard D. Brew and Co., Concord, NH. Model 14665-4.

§ Standard No. 640, NBS, Washington, DC, USA.

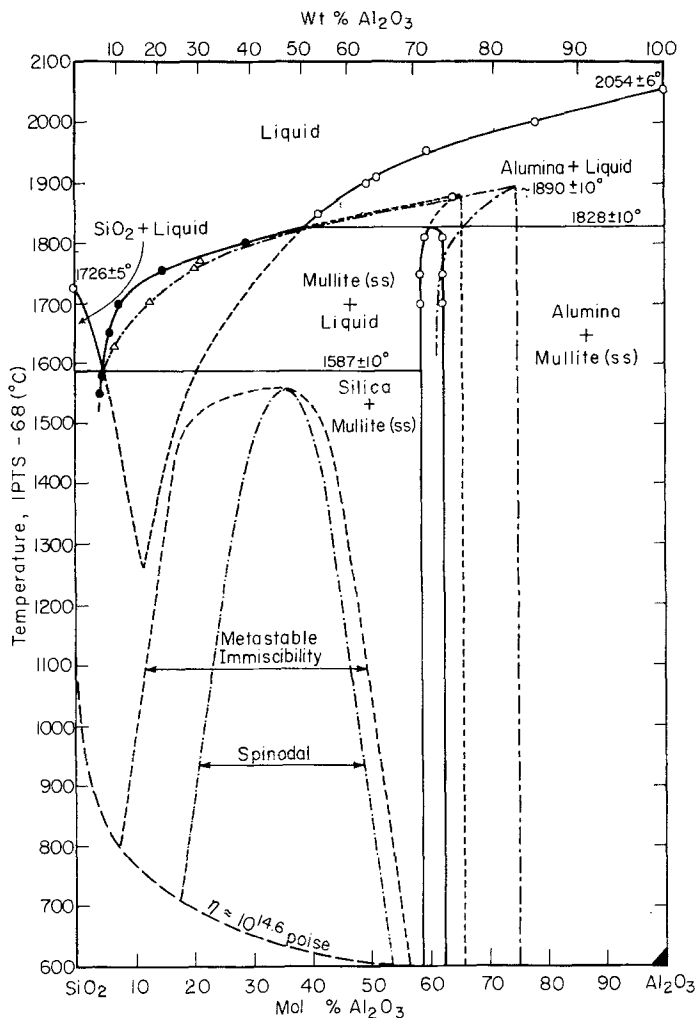


Figure 1 The extensions of the  $\text{SiO}_2$  (cristobalite) and  $\alpha\text{-Al}_2\text{O}_3$  (corundum) liquidi to form the metastable phase equilibrium diagram without mullite superimposed on the  $\text{SiO}_2\text{-Al}_2\text{O}_3$  phase equilibrium diagram reported by Aksay and Pask [2].

The molybdenum crucibles were cut on a diamond saw after the heat treatment and highly polished surfaces were prepared by ceramographic procedures. The polished sections were lightly etched in dilute HF and observed by interference contrast microscopy.\*

Samples for chemical analysis of the phases present in the microstructure were prepared by depositing a conducting carbon film on the polished sections and by painting the edges of the mounting material with a carbon-ethanol slurry. The samples were loaded into the vacuum chamber of the electron beam microprobe† and the primary characteristic X-ray intensities emitted from a specific phase in the microstructure were

compared with the emission from an identically coated standard of  $\text{Al}_2\text{O}_3$  and  $\text{SiO}_2$ . All measurements were made with an accelerating voltage of 15 kV at an X-ray emergence angle of  $41^\circ$ . The  $\text{AlK}\alpha$  and  $\text{SiK}\alpha$  intensities were simultaneously recorded on two spectrometers. Intensity counts in  $1\ \mu\text{m}$  steps starting with one phase and traversing across the various phases in the microstructure were monitored by logic circuit counters and simultaneously punched on IBM cards for data correction. Corrections for dead time, drift, background, absorption and fluorescence were made through a computer program adapted from Frazer *et al.* for use with the CDC-7600 computer system of this laboratory. Since the difference in atomic

\* Nomarski differential interference contrast Micrography, Zeiss Ultraphot II metallograph, Carl Zeiss, W. Germany.

† Materials Analysis Co., Palo Alto, Ca, USA.

numbers of Al and Si is small, no correction for atomic number was made.

### 3. Results and discussion

#### 3.1. Calculated metastable liquid

Calculated thermodynamic data for the  $\text{Al}_2\text{O}_3$  liquidus (Fig. 1), assuming  $\text{SiO}_2$  and  $\text{Al}_2\text{O}_3$  as the mixing components, are listed in Table I. These data were obtained from Equations 1 and 2 using experimentally reported values of the heat of fusion ( $25\,700\text{ cal mol}^{-1}$ ) and melting point ( $2323\text{ K}$ ) of  $\text{Al}_2\text{O}_3$ .

The activity coefficients  $\log_{10}\gamma_{\text{Al}_2\text{O}_3}$  listed in Table I were used to calculate isothermal activity coefficients at a particular temperature  $T$ . For example, at a temperature of  $1673\text{ K}$  the  $\log_{10}\gamma_{\text{Al}_2\text{O}_3}^L$  values calculated from Equation 2 were fitted by the least squares method to the expression:

$$\log_{10}\gamma_{\text{Al}_2\text{O}_3}^{1673} = (-0.187 + 2.05 X - 3.37 X^2 + 1.5 X^3)$$

where  $X$  = mole fraction of  $\text{Al}_2\text{O}_3$  ( $0.4 < X < 1.0$ ). Assuming that this expression is valid for  $\text{Al}_2\text{O}_3$  mole fractions less than 0.4, isothermal  $\log_{10}\gamma_{\text{Al}_2\text{O}_3}$  values at  $1673\text{ K}$  were obtained for  $\text{Al}_2\text{O}_3$  mole fractions between 0.15 and 0.35. These  $\log_{10}\gamma_{\text{Al}_2\text{O}_3}$  values, when used in Equations 1 and 2, yielded the temperatures of the metastable  $\text{Al}_2\text{O}_3$  liquidus in the mole fraction

TABLE I Thermodynamic data from  $\text{Al}_2\text{O}_3$  liquidus with  $\text{SiO}_2$  and  $\text{Al}_2\text{O}_3$  as mixing components

Mole fraction $\text{Al}_2\text{O}_3$ (Liquidus Composition)	Liquidus Temperature (K)	$\log_{10}\gamma_{\text{Al}_2\text{O}_3}$
1.00	2327	0.0000
0.95	2310	0.0087
0.90	2301	0.0226
0.85	2288	0.0335
0.80	2280	0.0512
0.75	2266	0.0639
0.70	2254	0.0806
0.65	2243	0.1004
0.60	2226	0.1159
0.55	2205	0.1293
0.50	2195	0.1590
0.45	2148	0.1478
0.40	2105	0.1444
0.30	2004	0.1382
0.25	1937	0.1195
0.20	1856	0.0090
0.15	1759	0.0047

range 0.15 to 0.35. Similar calculations were performed for the  $\text{SiO}_2$  liquidus. The calculated extensions of the  $\text{SiO}_2$  and  $\text{Al}_2\text{O}_3$  liquidus are shown in Fig. 1 superimposed on the stable and metastable equilibria proposed by Aksay and Pask [2]; a metastable binary eutectic is indicated at a  $\text{Al}_2\text{O}_3$  mole fraction of 0.12 (18 wt %) and  $1260^\circ\text{C}$ . The figure also shows the recently proposed miscibility gap [8].

#### 3.2. Subsolidus cristobalite—corundum reactions

The eutectic temperature of the metastable  $\text{SiO}_2$ — $\text{Al}_2\text{O}_3$  system was determined experimentally by firing cristobalite—corundum pellets and measuring the shrinkage. Table II summarizes the shrinkage data for a mixture containing  $\sim 27\text{ wt } \%$  ( $\sim 18\text{ mol } \%$ )  $\text{Al}_2\text{O}_3$ . No mullite formation was detected after firing, as determined by X-ray diffraction. However, the shrinkage of the compacts was increased considerably at firing temperatures above  $1250^\circ\text{C}$ . At  $1280^\circ\text{C}$  a linear shrinkage of  $\sim 13\%$  was observed. This sharp change in sintering characteristics from  $1250$  to  $1280^\circ\text{C}$  suggests the formation of some liquid phase which promotes sintering. Since liquid formation is to be expected at the eutectic temperature in the metastable  $\text{SiO}_2$ — $\text{Al}_2\text{O}_3$  system, the eutectic temperature from the above data is expected to be between  $1250$  and  $1280^\circ\text{C}$ . The correspondence of the calculated eutectic point with the experimental data of  $1260^\circ\text{C}$  is good. Furthermore, Staley and Brindley [4] reported an average composition of  $\text{Al}_2\text{O}_3 \cdot 5\text{SiO}_2$  ( $\approx 17\text{ mol } \%$   $\text{Al}_2\text{O}_3$ ) for the non-crystalline component formed in reactions between cristobalite and corundum

TABLE II Subsolidus reactions in cristobalite—corundum mixtures ( $\sim 27\text{ wt } \%$   $\text{Al}_2\text{O}_3$ ).

Temperature ( $^\circ\text{C} \pm 20$ )	Time (h)	Diameter of compacts (in.)		Linear shrinkage (%)
		Before firing	After firing	
1130	960	0.250	0.250	Pellet crumbled
1200	150	0.250	0.249	Pellet crumbled
1230	120	0.250	0.249	< 1
1250	120	0.250	0.248	1
1280	24	0.250	0.218	13

Crystalline phases after firing determined by X-ray diffraction:  $\alpha$ - $\text{Al}_2\text{O}_3$ , cristobalite.

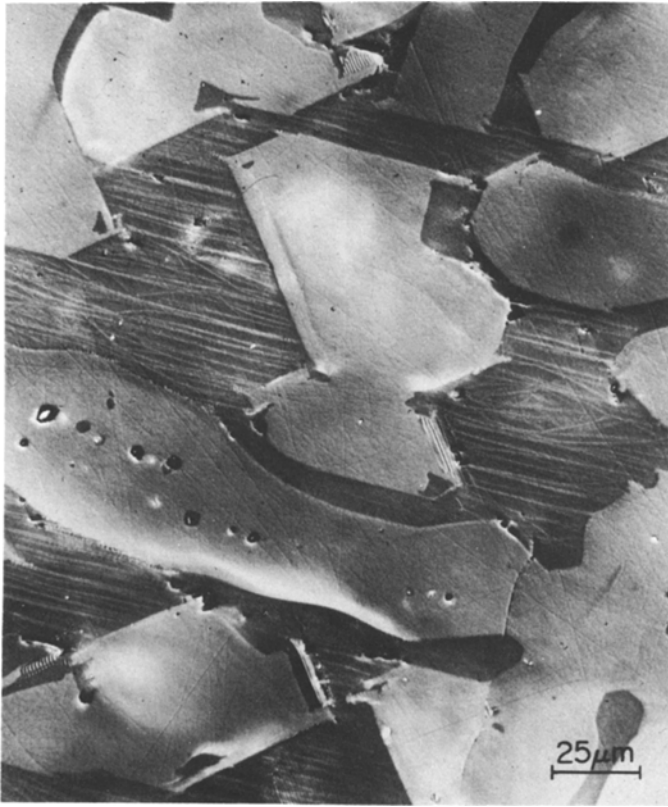


Figure 2 Microstructure of specimen containing 80 wt%  $\text{Al}_2\text{O}_3$  melted in sealed Mo crucible at  $\sim 1985^\circ\text{C}$  for 1.5 h cooled to  $1750^\circ\text{C}$  in 1 h, and quenched to room temperature [2]. Both large and needle-like precipitates are  $\alpha\text{-Al}_2\text{O}_3$  surrounded by a glassy matrix.

mixtures fired at  $1500^\circ\text{C}$ . This composition is very close to the  $\text{Al}_2\text{O}_3$  liquidus at  $1500^\circ\text{C}$  shown in Fig. 1.

### 3.3. microstructures of slowly cooled melts

A  $\text{SiO}_2\text{-Al}_2\text{O}_3$  melt containing 71 mol% (80 wt%)  $\text{Al}_2\text{O}_3$  was cooled from the homogenization temperature of  $\sim 1985^\circ\text{C}$  to  $1750^\circ\text{C}$  in 1 h to allow the precipitation and growth of  $\text{Al}_2\text{O}_3$  [2]; a rapid quench from the homogenization temperature always resulted in crystallization of mullite plus residual glass [2, 10]. The microstructure of the slowly cooled specimen is shown in Fig. 2. X-ray diffraction indicated the presence of  $\alpha\text{-Al}_2\text{O}_3$  as the only crystalline phase. An average composition of  $\approx 48\text{ wt}\% \text{Al}_2\text{O}_3$  ( $\sim 36\text{ mol}\% \text{Al}_2\text{O}_3$ ) was reported for the matrix surrounding the primary  $\text{Al}_2\text{O}_3$  precipitates. Since this average value was obtained by an electron microprobe scan of the matrix consisting of glass plus the fine  $\text{Al}_2\text{O}_3$  needles, it is likely to indicate a slightly higher  $\text{Al}_2\text{O}_3$  content than the actual glass composition. Consequently, the composition of the metastable  $\text{Al}_2\text{O}_3$  liquidus at  $1750^\circ\text{C}$  may be expected to be

slightly less than 48 wt%  $\text{Al}_2\text{O}_3$  ( $\sim 36\text{ mol}\% \text{Al}_2\text{O}_3$ ). The  $\text{Al}_2\text{O}_3$  liquidus obtained in the present work (Fig. 1) shows a composition of  $\approx 44\text{ wt}\% \text{Al}_2\text{O}_3$  ( $\sim 32\text{ mol}\% \text{Al}_2\text{O}_3$ ) at  $1750^\circ\text{C}$ .

The observations of Kennard *et al.* [5] also provided indirect evidence for the existence of a metastable  $\text{SiO}_2\text{-Al}_2\text{O}_3$  diagram. They solidified  $\text{SiO}_2\text{-Al}_2\text{O}_3$  ingots by the Bridgman technique. A 78 wt%  $\text{Al}_2\text{O}_3$  melt yielded a microstructure of glass plus crystalline  $\text{Al}_2\text{O}_3$ ; the glass composition was reported to be  $\sim 23\text{ wt}\% \text{Al}_2\text{O}_3$  ( $\sim 15\text{ mol}\% \text{Al}_2\text{O}_3$ ) on the basis of refractive index measurements. This composition lies at a temperature of  $\sim 1470^\circ\text{C}$  on the  $\text{Al}_2\text{O}_3$  liquidus shown in Fig. 1. The metastable  $\text{Al}_2\text{O}_3$  plus glass assemblage observed by Kennard *et al.* can thus be explained on the basis of the presented metastable diagram.

### 4. Summary

A metastable phase diagram between  $\text{SiO}_2$  (cristobalite) and  $\alpha\text{-Al}_2\text{O}_3$  (corundum) without mullite is proposed. The eutectic point of the diagram lies at a temperature of  $\approx 1260^\circ\text{C}$  at an  $\text{Al}_2\text{O}_3$  composition of  $\approx 18\text{ wt}\%$  ( $\approx 12\text{ mol}\%$ )  $\text{Al}_2\text{O}_3$ . The proposed diagram explains experimentally

observed reactions in cristabolite–corundum compacts and microstructures of slowly cooled  $\text{SiO}_2\text{--Al}_2\text{O}_3$  melts with high  $\text{Al}_2\text{O}_3$  contents.

### Acknowledgement

This work was supported by the Division of Basic Energy Sciences, US Department of Energy.

### References

1. R. F. DAVIS and J. A. PASK, *J. Amer. Ceram. Soc.* **55** (1972) 525.
2. I. A. AKSAY and J. A. PASK, *ibid.* **58** (1975) 507.
3. F. M. WAHL, R. E. GRIM and R. B. GRAF, *Amer. Mineral.* **46** (1961) 1064.
4. W. G. STALEY and G. W. BRINDLEY, *J. Amer. Ceram. Soc.* **52** (1969) 616.
5. F. L. KENNARD, R. C. BRADT and V. S. STUBICAN, "Reactivity of Solids", edited by J. S. Anderson (North Holland, Amsterdam, 1972) p. 580.
6. J. CHIPMAN, *Disc. Faraday Soc.* **4** (1948) 23.
7. M. REY, *ibid.* (1948) 257.
8. S. H. RISBUD and J. A. PASK, *J. Amer. Ceram. Soc.* **60** (1977) 418.
9. R. J. CHARLES, *ibid.* **60** (1967) 631.
10. S. H. RISBUD and J. A. PASK, *ibid.* **61** (1978) 63.

Received 31 January and accepted 3 March 1978.